Eur. Phys. J. D **12**, 45–51 (2000)

THE EUROPEAN PHYSICAL JOURNAL D

EDP Sciences

Spectrum of two quasiequal-energy electrons ejected by a high-energy photon

M.A. Kornberg[1,a] and J.E. Miraglia[2]

[1] Max-Planck-Institut für Quantenoptik, Hans-Kopfermann-strasse 1, 85748 Garching, Germany
[2] Instituto de Astronomía y Física del Espacio, Casilla de Correo 67, Sucursal 28, 1428 Buenos Aires, Argentina

Received 24 January 2000

Abstract. We present numerical results for the photoelectron spectrum in double ionization by keV photons in the quasiequal-energy sharing region. In this region of the spectrum, the relevant ionizing mechanism is due to a mutual sharing of the photon momentum by both electrons, with small momentum transferred to the atomic nucleus. Calculations were performed for photon energies of 25 and 50 keV, where retardation effects are fundamental, while final-state correlations are of minor importance. The spectra present a two-peak structure, with maxima located at the photoelectron energies $\epsilon_1 = \omega/2 \pm \sqrt{\omega^3/8c^2}$, with ω the photon energy in atomic units. We discuss the general features of the spectrum in terms of the picture of the photoionization of two free electrons, and we propose a way of detecting the contribution by experiments.

PACS. 32.80.Fb Photoionization of atoms and ions – 33.60.-q Photoelectron spectra

1 Introduction

In recent years there has been an active interest towards understanding processes of interaction of keV photons with atomic targets. Much of this interest has been generated by experiments conducted on modern synchrotron radiation sources (for a review, see *e.g.* Ref. [1]). Among the most recent experiments of this type we may cite:

(i) the measurement of the Compton ratio of double-to-single ionization of He in the photon-energy range 40–100 keV [2];
(ii) measurements of differential X-ray scattering cross-sections in Ne and He in the range 11–22 keV [3];
(iii) the double K-vacancy production in Mo by 50 keV photons [4].

These are only examples of the present state-of-the-art in the technology of synchrotron sources used for the investigation of atomic samples interacting with X-ray radiation.

In particular, the experiment of Spielberger *et al.* [2] is of interest here, since we will consider double ionization of He by keV photons. Nevertheless, our concern in this paper is on the photoabsorption process rather than on the Compton scattering process. It is well established that at sufficiently high photon energies the Compton process dominates over photoabsorption both for single and double ionization. The energy at which the cross-sections of both processes are approximately equal is about 6.3 keV [5]. Therefore, in the experiment of reference [2] ion-yield measurements (both He^+ and He^{2+}) are signatures of Compton scattering ionization, not photoabsorption. It is worth noting that the experiment of reference [2] was performed using the COLTRIMS technique (cold target recoil ion momentum spectroscopy [6]), in which the momentum distribution of recoiling nucleus is measured. Compton ions are left with small momentum ($p_n \sim 0$), and a plot of the momentum distribution of the recoiling nucleus in a plane perpendicular to the photon beam shows a large concentration around the very center. If a ring at a distance $p_n \sim \sqrt{2\omega}$ from the center had been observed as well, photoabsorption ions would have been recorded, since the photoabsorption process imparts large momentum to the ion [6]. There exists another photoabsorption mechanism leading to small momentum transferred to the nucleus ($p_n \sim 0$). This mechanism, in which we are concerned in the present work, results in the quasiequal-energy sharing by both electrons, which are ejected in nearly opposite directions.

In a recent paper [7], we have provided an estimate of the contribution of quasiequal-energy electrons on the total cross-section for double photoionization. We have shown that, for high energies, the main contribution to the cross-section comes from a non-dipole term called the quasifree contribution [8, 9]. The name for this contribution comes from the fact that, for high-energy photons, the two ejected electrons can be treated as quasifree [8]. Since in our case the electrons are indeed bounded to the nucleus, all departures from a quasifree picture are due to the momentum distribution of the electron pair in the atom before the interaction. In reference [7] we also showed

[a] e-mail: mjk@mpq.mpg.de

that there exists another contribution to the cross-section with dipole-like character, which decreases sufficiently fast as the photon energy increases. At 100 keV all the contribution is mainly non-dipole, and adds about 17% to the photoabsorption cross-section that comes from the asymmetric energy sharing (*i.e.* the shake-off process [10]).

The aim of this paper is to present numerical results for the spectrum in the quasiequal-energy sharing region. In particular, we show that the spectrum presents a two-peak structure, indicating that the electrons are mainly ejected with lightly different energies. Our results agree with the picture obtained from that of two free electrons, in that the structure of the spectrum could be analyzed in terms of energy and momentum conservation of two free electrons [9]. We explicitly show that the two-peak structure of the spectrum could not be accounted for in dipole approximation. The use of ground-state wave functions not having a cusp at the $e-e$ relative coordinate can not account for quasiequal-energy ejection, since the process can take place when the electrons are close to each other. Atomic units are used throughout except as otherwise stated.

2 Formulation

We consider the absorption of a high-energy photon of energy ω leading to ionization of two electrons. The transition matrix for this process reads

$$T = \langle \psi_{\rm f}^{-} | \hat{H}_{\rm rm} | \psi_{\rm i} \rangle, \tag{1}$$

where $\psi_{\rm i}(\mathbf{r}_1, \mathbf{r}_2)$ and $\psi_{\rm f}^{-}(\mathbf{k}_1, \mathbf{k}_2 | \mathbf{r}_1, \mathbf{r}_2)$ are the initial (bound) and final (double-continuum) helium wave functions, respectively. Here $\mathbf{k}_1$ and $\mathbf{k}_2$ are used to denote the electron momenta. The radiation-matter operator reads

$$\hat{H}_{\rm rm} = \exp(\mathrm{i}\mathbf{k}\cdot\mathbf{r}_1)\hat{\mathbf{e}}\cdot\nabla_{\mathbf{r}_1} + \exp(\mathrm{i}\mathbf{k}\cdot\mathbf{r}_2)\hat{\mathbf{e}}\cdot\nabla_{\mathbf{r}_2}, \tag{2}$$

where $\mathbf{r}_1$ and $\mathbf{r}_2$ are the coordinates of the electrons with respect to the heavy nucleus of charge $Z = 2$, $\hat{\mathbf{e}}$ is the polarization unit vector, $\mathbf{k}$ is the photon momentum ($\hat{\mathbf{e}}\cdot\mathbf{k} = 0$), $k = \omega/c$, and c is the speed of light.

In this work we consider the particular case of quasiequal-energy electrons, which are mainly ejected in opposite directions. Since the photon energy is very high, quasiequal-energy electrons are ejected each with high energy, and final-state correlations should be of minor importance. Therefore, these fast electrons will be described by using a plane-wave representation

$$\psi_{\rm f}^{-}(\mathbf{k}_1, \mathbf{k}_2 | \mathbf{r}_1, \mathbf{r}_2) = \frac{[1 + \mathcal{P}_{12}]}{(2\pi)^3\sqrt{2}} \exp\left(\mathrm{i}\mathbf{k}_1\cdot\mathbf{r}_1 + \mathrm{i}\mathbf{k}_2\cdot\mathbf{r}_2\right), \tag{3}$$

where $\mathcal{P}_{12}$ is the exchange operator. Equation (3) should be valid for $k_1 \sim k_2 \sim \sqrt{\omega} \gg Z$, *i.e.* where the Coulomb interactions are expected to give a small contribution.

The transition matrix, using the plane-wave representation, can be expressed in the form

$$T = \mathrm{i}\sqrt{2}\left[\hat{\mathbf{e}}\cdot\mathbf{k}_1\tilde{\psi}_{\rm i}(\mathbf{k}_1 - \mathbf{k}, \mathbf{k}_2) + \hat{\mathbf{e}}\cdot\mathbf{k}_2\tilde{\psi}_{\rm i}(\mathbf{k}_1, \mathbf{k}_2 - \mathbf{k})\right], \tag{4}$$

where $\tilde{\psi}_{\rm i}$ is the double-Fourier-transform given by

$$\tilde{\psi}_{\rm i}(\mathbf{p}_1, \mathbf{p}_2) = \iint \frac{\mathrm{d}\mathbf{r}_1\mathrm{d}\mathbf{r}_2}{(2\pi)^3} \exp\left(-\mathrm{i}\mathbf{p}_1\cdot\mathbf{r}_1 - \mathrm{i}\mathbf{p}_2\cdot\mathbf{r}_2\right) \times \psi_{\rm i}(\mathbf{r}_1, \mathbf{r}_2). \tag{5}$$

Once we have written down the amplitude (Eq. (4)), the process is then described by the basic observable referred to as the five-fold differential cross-section (5DCS)

$$\frac{\mathrm{d}^5\sigma^{2+}}{\mathrm{d}\epsilon_1\mathrm{d}\Omega_1\mathrm{d}\Omega_2} = \frac{4\pi^2}{\omega c}k_1k_2|T|^2. \tag{6}$$

In the last equation ϵ_1 is the energy of the electron detected within the angular range given by $\mathrm{d}\Omega_1$, while the energy of the second electron is fixed by energy conservation $\epsilon_1 + \epsilon_2 = \omega + \epsilon_0$, with ϵ_0 the ground-state energy. The second electron is detected within the angular range $\mathrm{d}\Omega_2$. Since we are in a high-energy case $\omega \gg -\epsilon_0$, the total-available energy $\omega + \epsilon_0 \simeq \omega$.

To calculate the transition matrix (Eq. (4)) we need to specify the initial-state wave function, which is considered to be of the form

$$\psi_{\rm i}(\mathbf{r}_1, \mathbf{r}_2) = N_1\psi_0(\mathbf{r}_1, \mathbf{r}_2) - N_1\delta\psi_0(\mathbf{r}_1, \mathbf{r}_2)\mathrm{e}^{-\gamma r}, \tag{7}$$

with $\psi_0(\mathbf{r}_1, \mathbf{r}_2) = \mathrm{e}^{-\alpha r_1 - \beta r_2} + \mathrm{e}^{-\beta r_1 - \alpha r_2}$ and $\mathbf{r} = \mathbf{r}_1 - \mathbf{r}_2$. We have optimized the parameters of this wave function by minimizing the bound-state energy (ϵ_0), and imposing that $\delta\gamma/(1-\delta) = 1/2$. This condition is required to satisfy the Kato cusp condition [11] at the coalescence point $r = 0$, namely

$$\left(\frac{\partial\psi_{\rm i}}{\partial r}\right)_{r=0} = \frac{1}{2}\psi_{\rm i}(r = 0). \tag{8}$$

Equation (8) is referred to as the 2nd Kato cusp condition, the 1st Kato condition being that at the electron-nucleus ($e-n$) coordinate,

$$\left(\frac{\partial\psi_{\rm i}}{\partial r_j}\right)_{r_j=0} = -Z\psi_{\rm i}(r_j = 0), \qquad j = 1, 2. \tag{9}$$

The values of the calculated parameters are: $N_1 = 1.2959$, $\alpha = 1.4037$, $\beta = 2.2069$, $\gamma = 0.4504$, and $\delta = 0.5261$. With these parameters, our wave function accounts for 94.4% of the correlation energy. If instead of requiring the fulfillment of equation (8), we had determined the parameters by minimizing the energy ϵ_0 and allowing the coefficients to vary freely, the wave function so obtained would account for 96% of the correlation energy, while the 2nd Kato cusp condition (Eq. (8)) would be 0.74 instead of 0.5. However, we should remark that the 2nd Kato condition

is the most sensitive magnitude to be fulfilled by the wave function for the process here studied, since quasiequal-energy electrons are ejected when they are close to each other before the interaction. As we will see in Section 4, if we attempt to calculate quasiequal-energy ejection by using a wave function without a cusp at $r = 0$, no enhancement of the cross-section will be observed. The Kato cusp condition at the electron-nucleus coordinate is not of importance here; it must be considered when the electrons are ejected with highly asymmetric energy sharing, *i.e.* the shake-off process.

3 Numerical computations

In this section we describe the method used for the numerical calculation of the spectrum. For that, we need to calculate the transition matrix (Eq. (4)) with the initial state (Eq. (7)) in the momentum space. Using equation (5), we write equation (7) in Fourier space

$$\tilde{\psi}_{\rm i}(\mathbf{p}_1,\mathbf{p}_2) = N_1\tilde{\psi}_0(\mathbf{p}_1,\mathbf{p}_2) - N_1\delta\int\frac{{\rm d}\mathbf{K}}{\pi^2}\frac{\gamma}{(\gamma^2+K^2)^2}\tilde{\psi}_0(\mathbf{p}_1-\mathbf{K},\mathbf{p}_2+\mathbf{K}), \quad (10)$$

where

$$\tilde{\psi}_0(\mathbf{p}_1,\mathbf{p}_2) = (1+\mathcal{P}_{12})\,\frac{8}{\pi}\frac{\alpha}{(\alpha^2+\mathbf{p}_1^2)^2}\frac{\beta}{(\beta^2+\mathbf{p}_2^2)^2}\,. \quad (11)$$

We have performed a full numerical calculation using the exact solution of the integral appearing in equation (10). In reference [7] the evaluation of the contribution of quasiequal-energy electrons was done using the peaking approximation for the Fourier transform of the initial state, which is valid for $\mathbf{p}_1 \sim -\mathbf{p}_2$, and $p_1, p_2 \gg Z$. We undertake here the exact calculation. To that end, we have considered the Lewis-type three denominator integral

$$\mathcal{J}_{n_1,n_2,n_3} = \int{\rm d}\mathbf{x}\prod_{j=1}^{3}\frac{1}{\left[a_j^2+(\mathbf{x}-\mathbf{s}_j)^2\right]^{n_j}}\,, \quad (12)$$

with $\mathbf{s}_1 = \mathbf{p}_1$, $\mathbf{s}_2 = -\mathbf{p}_2$, and $\mathbf{s}_3 = \mathbf{0}$. The integral in equation (10) is given by $\mathcal{J}_{2,2,2}$, which is related to $\mathcal{J}_{1,1,1}$ through the following parametric derivation

$$\mathcal{J}_{2,2,2} = -\frac{1}{2^3}\prod_{j=1}^{3}\frac{1}{a_j}\frac{\partial}{\partial a_j}\mathcal{J}_{1,1,1}. \quad (13)$$

Therefore, we were able to evaluate analytically the matrix element (Eqs. (4, 10)) since $\mathcal{J}_{1,1,1}$ is known in closed form [12]:

$$\mathcal{J}_{1,1,1} = \frac{\pi^2}{Q}\ln\left[\frac{S+Q}{S-Q}\right] \quad (14)$$

with

$$Q = \sqrt{S^2-T}, \quad (15)$$

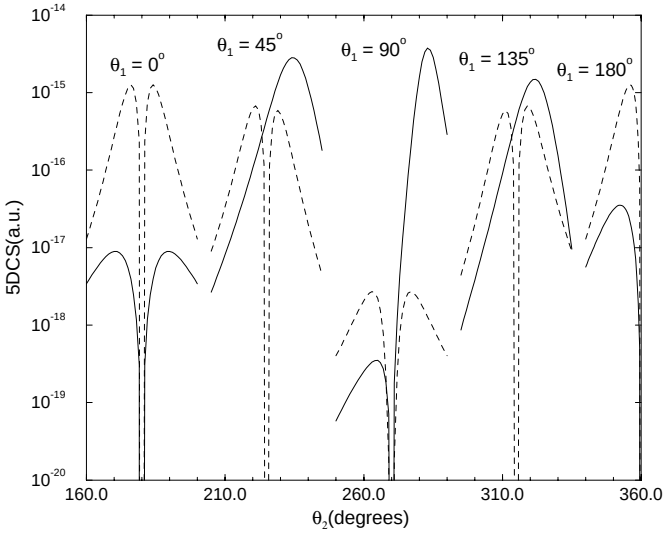

Fig. 1. The 5DCS calculated at the photon energy $\omega = 25$ keV, and for equal-energy sharing ($\epsilon_1 = \epsilon_2$). The geometry was chosen such that $\mathbf{k} = k\hat{\mathbf{z}}$ and $\hat{\mathbf{e}} = \hat{\mathbf{x}}$. The calculations were done for $\varphi_1 = \varphi_2 = 0^\circ$, *i.e.* in the plane defined by $\mathbf{k}$ and $\hat{\mathbf{e}}$. Results are shown at various angles for the ejection of the first electron (electron 1), and we only plot the cross-section near the values $\theta_2 \sim \theta_1 + 180^\circ$, since for values away from back-to-back emission the cross-section drops abruptly. The solid lines are the calculations including full retardation, while the dashed lines are the results within dipole approximation.

$$T = [(\mathbf{p}_1+\mathbf{p}_2)^2+(a_1+a_2)^2][\mathbf{p}_1^2+(a_1+a_3)^2] \times [\mathbf{p}_2^2+(a_2+a_3)^2], \quad (16)$$

and

$$S = [(\mathbf{p}_1+\mathbf{p}_2)^2+(a_1+a_2)^2]a_3 + [\mathbf{p}_1^2+a_1^2+a_3^2]a_2 + [\mathbf{p}_2^2+a_2^2+a_3^2]a_1. \quad (17)$$

The derivatives are tedious to perform, but at the end $\mathcal{J}_{2,2,2}$ can be obtained in (large) closed form.

Once the matrix element has been calculated, the photoelectron spectrum was obtained integrating over the four angular coordinates (Ω_1, Ω_2) in equation (6) using a Monte-Carlo algorithm. The relative error for the integration was set in 8%. It was not possible to obtain converged results with a relative error less than this value, since the integrand peaks strongly within a very narrow region in momentum space. We should note that the numerical results presented in the next section agree, within the numerical accuracy, with those obtained through the use of the peaking approximation [7].

To show the sharp integrand peaks, we plot in Figure 1 the 5DCS at 25 keV for the case of equal-energy sharing ($\epsilon_1 \equiv \epsilon_2$), in the plane defined by $\mathbf{k}$ and $\hat{\mathbf{e}}$. The plot shows the cross-section at different angles for the observation of the first electron (electron 1). The main contribution comes from a small range of angles for the second electron θ_2, typically within a range of 30 degrees. We only plot the

cross-section within this range, since for other angles θ_2 the cross-section decreases abruptly. There are other features of interest in the results of Figure 1. Within dipole approximation (dashed line) the cross-section is zero at $\theta_2 \equiv \theta_1 + 180°$. This comes from a selection rule valid within dipole approximation, *i.e.* $T(\mathbf{k} = 0, \mathbf{k}_1, -\mathbf{k}_1) = 0$. Although we have used here a plane-wave final state, this selection rule is general and valid for exact wave functions [13]. In the general case (solid line), a zero in the cross-section appears when $\mathbf{k}_1$ is in the direction of $\hat{\mathbf{e}}$ or $\mathbf{k}$ and $\mathbf{k}_1 \equiv -\mathbf{k}_2$. Although the cross-section cuts abruptly in this case, peaks strongly and even surpass in magnitude the dipole-case results. It is of interest to note that the peak-structure of the cross-section, which is concentrated around the configuration $\mathbf{k}_1 \sim -\mathbf{k}_2$, is a direct manifestation of ground-state correlation, here embedded into the 2nd Kato cusp condition.

4 Results and discussion

In this section, we present and discuss our results for the photoelectron spectrum in the quasiequal-energy sharing region. To begin with, we should mention a couple of points about the physics of the process. For high-energy photon impact, ejection of two electrons with similar energies is allowed when these electrons are close to each other. Further, if the electrons are somewhat away from the nucleus, we may treat them as been quasifree [8], provided that the photon energy is very high, $\omega \gg -\epsilon_0$. Let we think for a moment in two free electrons interacting with a high-energy photon. The photon momentum is assumed to be in the z-direction. After the interaction, energy ($\epsilon_1 + \epsilon_2 = \omega$) and momentum ($\mathbf{k}_1 + \mathbf{k}_2 = \mathbf{k}$) conservation mandate that the electron energies must be given, with very good accuracy, by

$$\epsilon_1 = \frac{\omega}{2} \pm \frac{\omega^{3/2}}{2c} \cos\theta_1, \tag{18}$$

and $\epsilon_2 = \omega - \epsilon_1$. Electrons should have equal energies when ejected at right angles with the photon beam, while the maximum asymmetry in energy sharing should take place when ejected in the same direction of the photon beam. From the preceding equation, we obtain that the electron energies should be in the range [9]

$$|\epsilon_1 - \epsilon_2| \leq \frac{\omega^{3/2}}{c} \cdot \tag{19}$$

The picture of two free electrons is not exactly applied to our present problem, since the electrons are bounded to the nucleus through the Coulomb potential and are interacting with each other. Nevertheless, this simple picture will help us to explain some features of the photoelectron spectrum here presented. We should note that the equations for energy and momentum conservation given above are still valid in our case provided we assume that the momentum transferred to the nucleus is very small, *i.e.* $k \gg p_n$ with p_n the momentum transferred to the nucleus.

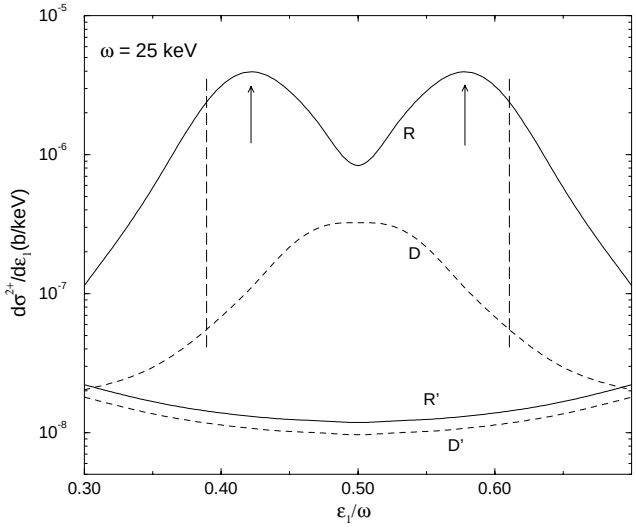

Fig. 2. Photoelectron energy spectrum in the quasiequal-energy region for the photon energy $\omega = 25$ keV. The final state is described by a plane-wave representation (Eq. (3)), while the initial state is given by equation (7) with coefficients determined to satisfy the 2nd Kato cusp condition (see text). Solid line labeled R: full calculation including retardation. Dashed line labeled D: calculation within dipole approximation. Solid line labeled R′: full calculation including retardation with initial state with $\delta = 0$. Dashed line labeled D′: calculation within dipole approximation with initial state with $\delta = 0$. The calculations with $\delta = 0$ were done with coefficients recalculated so the wave function to be normalized; these calculations give no trace of quasiequal-energy sharing, since the wave function in this case has no cusp at $r = 0$. The vertical dashed lines mark the range of energies allowed for two-free electrons (Eq. (19)), while the vertical arrows are the maxima determined from equation (20).

In Figure 2 we present the spectrum in the quasiequal-energy region at the photon energy of 25 keV, calculated numerically as explained in Section 3. The vertical dashed lines mark the maximum range of energies allowed for two free electrons, as given by equation (19). Our spectra extend out of these limits, since these are physical limits valid only in the idealized case of two free electrons, or conversely in the limit of infinite photon energy. The solid line in Figure 2 labeled R is our final result for the spectrum. It presents a two-peak structure and a dip at the very center. We will discuss first this curve, and afterwards we will make the presentation and analysis of the other three curves in that figure. Note first that the main contribution to the spectrum is well within the limits imposed by the two-free electron case. Out of these limits the cross-section falls abruptly, and makes almost not relevant contribution to the total yield. The two peaks in the spectrum could be accounted for in the following manner. At this photon energy, two-electron ejection with quasiequal energies is mainly a non-dipolar process, also referred to as quasifree [8]. The quasifree contribution,

which is of quadrupole character, has the angular dependence $\sin^2\theta_q\cos^2\theta_q$ on the angle $\theta_q = \cos^{-1}(\hat{\mathbf{q}}\cdot\hat{\mathbf{k}})$ (see Eq. (11) of Ref. [7]). Here $\mathbf{q}$ denotes the relative momentum of the electrons, $\mathbf{q} = (\mathbf{k}_1 - \mathbf{k}_2)/2$. The maximum probability for the ejection of the electron pair is therefore at 45 degrees with respect to the direction of the photon momentum. Using this result into equation (18), we conclude that the electrons should be ejected with higher probabilities with energies

$$\epsilon_1 = \frac{\omega}{2} \pm \sqrt{\frac{\omega^3}{8c^2}}\,. \tag{20}$$

This explains quite well the positions of the two peaks observed in our results (curve labeled R) in Figure 2. The values given by equation (20) are marked in Figure 2 as the vertical arrows. Although the mechanism leading to the ejection of two fast electrons, when considering retardation, produces a pair of quasiequal-energy electrons, the maximum probability is for the ejection of the electron pair in a lightly asymmetric form, the difference in energy sharing being roughly 4 keV for the initial photon energy of 25 keV.

We discuss now the other three curves presented in Figure 2. The curve labeled D in that figure is the result of using the dipole approximation. Note that it is of smaller magnitude, and that there is only one peak at the very center. The smaller magnitude is due to the fact that the quasifree contribution, being of non-dipole character, is absent. The quasifree contribution dominates the ejection of electrons of similar energies for high-photon energies, and this contribution could only be accounted for in a calculation that goes beyond dipole approximation. The other feature of the spectrum, of having only one peak at the very center, is also a fact of neglecting the photon momentum within the dipole calculation. We have made above an analysis in terms of energy and momentum conservation for two free electrons. If in that analysis we would consider $k = 0$, we obtain that the electrons should be ejected with *exactly* equal energies and in opposite directions. This explains the maximum observed in Figure 2 at $\epsilon_1 = \omega/2$ for the curve labeled D.

Finally, we present in Figure 2 two other curves labeled R′ and D′, which correspond to calculations including retardation (R′) and in dipole approximation (D′). These curves were obtained by setting $\delta = 0$ in equation (7). In this case there is no increase or structure in the cross-section in the central region in none of both calculations. This is due to the fact that, when setting $\delta = 0$, the initial state does not have a cusp at the coalescence point $r = 0$. The initial-state wave function does not account for the $e-e$ interaction, and the ejection of electrons with similar energies could not be taken into account when using this initial-state. It could be further easily proved that, if we write the initial state as $\psi_{\rm i}(\mathbf{r}_1, \mathbf{r}_2) = \phi_0(r_1)\phi_0(r_2)$, the Fourier-transform (Eq. (5)) of that state behaves asymptotically as $\tilde{\psi}_{\rm i} \propto q^{-8}$, when the relative momentum of the electrons $q \to \infty$. This corresponds to the first term on the right-hand side of equation (10). To obtain the contribution from quasiequal-energy sharing the initial state employed should have the proper behavior $\tilde{\psi}_{\rm i} \propto q^{-4}$ [7], as is the case for the initial state of equation (10) due to the second term on the right-hand side.

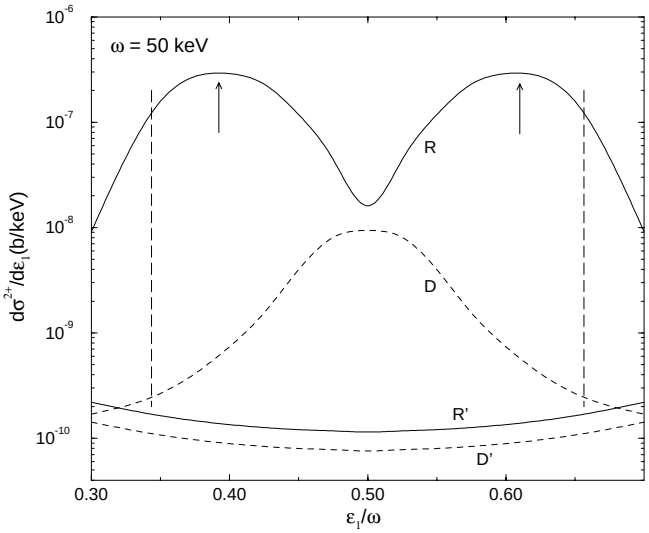

Fig. 3. As Figure 2, but for the photon energy $\omega = 50$ keV.

In Figure 3 we present the photoelectron spectrum at a higher photon energy $\omega = 50$ keV. The various analysis we have made at 25 keV are also valid here. Some few comments are only necessary. At 50 keV the difference in magnitude between the curves R and D is more pronounced, since as was already shown, the total yield for curve R falls off as $\omega^{-5/2}$, while for curve D falls off as $\omega^{-9/2}$ [7]. The peak maxima in curve R are now at different energies than in the previous case (Fig. 2), which are again well accounted for by equation (20). The two peaks are now more away from the midpoint. As the photon energy increases, the two peaks of the spectrum predicted by equation (20) move towards the shake-off regions placed at $\epsilon_1 \sim 0$ and $\epsilon_1 \sim \omega$. The limits $\epsilon_1 \sim 0$ and $\epsilon_1 \sim \omega$ in equation (20) occur when $\omega \sim 2c^2 \sim 1$ MeV. At these impact energies, however, the non-relativistic formalism employed here looses significance. We should stress that our results are valid for non-relativistic energies ($\omega \ll c^2$). It is of interest to note, that similar characteristics in the shape of the spectrum (curve labeled R) were found in [8,9] by using other approaches. Those calculations, performed at different photon energies than the ones here addressed, will be compared with results using our method in a future work.

We have presented calculations of the spectrum within the energy range $0.3 < \epsilon_1/\omega < 0.7$, which is the relevant region for the ejection of quasiequal-energy electrons for the photon energies here considered. However, we have not presented those curves in the shake-off regions (*i.e.* $\epsilon_1 \sim 0$ and $\epsilon_1 \sim \omega$). The reason is that the final-state used here is adequate for describing two fast electrons moving in opposite directions, but is not adequate to represent the physical situation of shake-off, in which the energy asymmetry between the electrons is almost complete. Our results for the four different calculations in Figures 2 and 3

give nearly equal results in the shake-off region, the difference being of order $2\omega/c^2$ between R and D curves for the same initial state. However, the magnitude of the spectra in the shake-off region is not correctly predicted when using the plane-wave final state.

The ejection of quasiequal-energy electrons is a peculiar effect of the electron-electron interaction, but this effect has not been observed experimentally yet. It is then necessary to inquire if the predictions we have done here could confront an experimental verification. As was already pointed out [7], observation of recoil ions carrying small momentum ($p_n \sim 0$) produced by quasiequal-energy sharing is not feasible. The reason is that ions with small momentum are mainly produced by the Compton scattering process, about 4 orders of magnitude larger [14]. The only possibility then rests in the observation of the fast electrons produced by quasiequal-energy sharing. To be more specific, let us consider a photon beam of 50 keV. In this case, electrons ejected by single-photoionization should have energies close to 50 keV, as well as the fast electron produced in double ionization by the shake-off mechanism. The main contribution to Compton ionization comes for energies transferred less than the binary encounter energy $\Delta E \sim 2\omega^2/c^2$, which for 50 keV primary photons is about $\Delta E \sim 10$ keV. The Compton process produces electrons, with higher probability, with energies lower than 10 keV. The probability of producing electrons of energies larger than 10 keV by the Compton process is highly reduced, since the cross-section drops abruptly for energies transferred above the binary encounter energy [15,16]. From equation (20), electrons produced by quasiequal-energy sharing will be mainly ejected with energies close to 19.5 keV and 30.5 keV. Compton ionization could not account for the production of these high-energy electrons. Therefore, observation of these fast electrons should be an unmistakable signature of the process studied in the present work. Further, such a measurement would not require to be done in coincidence, since there is no other competitive process to account for the production of these fast electrons. In summary, detection of fast electrons with energies close to those predicted by equation (20), most likely at 45 degrees with respect to the direction of the photon beam, should be the most favorable situation for the observation of electrons produced by quasiequal-energy sharing process.

To end this section, we wish to make a few comments on results that we published in previous works [17,18]. In reference [17] we reported calculations showing a bump in the photoelectron spectrum at the center of the energy distribution. Those calculations were performed within dipole approximation for $\omega = 2$ keV and 3 keV. The calculations presented here in Figures 2 and 3 at higher photon energies also show this kind of structure within dipole approximation. The difference between the present calculations and those in reference [17] rests in that we have used here plane-waves for the final state, while in reference [17] a correlated final state was employed. However, it is not expected that uncorrelated final states give a good account for the magnitude of the spectrum in the central region at low photon energies (between 2 and 10 keV). Use of planes waves is justified for high energies, where the process can be considered to be truly impulsive. At lower photon energies, in the range 2–10 keV, it is necessary to consider effects coming from final-state interaction. At those low energies retardation effects are small, while final-state correlations are more important. The approximations used in the present work, valid for substantially higher energies, are in fact on the opposite side: retardation effects are the most relevant, while final-state correlations are of little importance. Other calculations, using highly-correlated configuration-interaction-type (CI-type) wave functions, presented in reference [17] at 3 keV, and at a higher photon energy ($\omega = 12$ keV) in reference [18], failed to describe any enhancement or structure in the central region of the spectrum. The reason is that the CI-type wave function used in those works does not account adequately for the $e-e$ interaction when the electrons are close to each other, while describes very well the energy eigenvalue and the $e-n$ interaction through the 1st Kato cusp condition (Eq. (9)).

5 Summary and conclusions

In this work we have studied the photoelectron spectrum in two-electron ionization by keV photons in the quasiequal-energy sharing region. This region of the spectrum is characteristically different from the shake-off region, in which the electrons share the energy in a highly asymmetric form. The physical mechanisms for ionization in these two regions of the spectrum are also different. In the shake-off region the slow electron is promoted into the continuum by loss of screening, sometimes also referred to as the projection of the wave function. In the quasiequal-energy region, the process takes place by the mutual sharing of the photon momentum by both electrons, which are ejected at almost back-to-back angles [8]. In this process almost no net momentum is transferred to the atomic nucleus [9].

We have shown that, in the central region of the spectrum, the energy distribution is determined by a lightly asymmetric energy sharing. However, each electron carries a substantial amount of the total energy. This scenario is well accounted for by the picture of two free electrons, since in the process studied here the momentum transferred to the nucleus is of minor importance. Our results were obtained numerically, and the integrated spectra agree quite well with analytic results presented previously [7]. Finally, we have proposed a way for measuring the contribution coming from quasiequal-energy sharing. The analysis was done for helium, but a similar situation is expected to be found in other atoms. In particular, a comparative study for two-electron systems will be presented elsewhere [19].

This work has been partially supported under Grant No. PIP-4401 (CONICET). The work of M.A.K. has been supported by the Argentina Research Council. One of us (M.A.K.) would like to thank J. Burgdörfer and L. Spielberger for useful discussions.

References

1. B. Crasemann, Can. J. Phys. **76**, 251 (1998).
2. L. Spielberger, H. Bräuning, A. Muthig, J.Z. Tang, J. Wang, Y. Qiu, R. Dörner, O. Jagutzki, Th. Tschentscher, V. Honkimäki, V. Mergel, M. Achler, Th. Weber, Kh. Khayyat, J. Burgdörfer, J. McGuire, H. Schmidt-Böcking, Phys. Rev. A **59**, 371 (1999).
3. M. Jung, R.W. Dunford, D.S. Gemmell, E.P. Kanter, B. Krässig, T.W. LeBrun, S.H. Southworth, L. Young, J.P.J. Carney, L. LaJohn, R.H. Pratt, P.M. Bergstrom Jr, Phys. Rev. Lett. **81**, 1596 (1998).
4. E.P. Kanter, R.W. Dunford, B. Krässig, S.H. Southworth, Phys. Rev. Lett. **83**, 508 (1999).
5. D.V. Morgan, R.J. Bartlett, Phys. Rev. A **59**, 4075 (1999).
6. J. Ullrich, R. Moshammer, R. Dörner, O. Jagutzki, H. Schmidt-Böcking, L. Spielberger, J. Phys. B **30**, 2917 (1997).
7. M.A. Kornberg, J.E. Miraglia, Phys. Rev. A **60**, R1743 (1999).
8. M. Ya Amusia, E.G. Drukarev, V.G. Gorshkov, M.P. Kazachkov, J. Phys. B **8,** 1248 (1975).
9. E.G. Drukarev, Phys. Rev. A **52**, 3910 (1995).
10. A. Dalgarno, H.R. Sadeghpour, Phys. Rev. A **46**, R3591 (1992).
11. T. Kato, Commun. Pure Appl. Math. **10**, 151 (1957).
12. R.R. Lewis, Phys. Rev. **102**, 537 (1956).
13. Z. Teng, R. Shakeshaft, Phys. Rev. A **49,** 3597 (1994).
14. B. Krässig, R.W. Dunford, D.S. Gemmell, S. Hasegawa, E.P. Kanter, H. Schmidt-Böcking, W. Schmitt, S.H. Southworth, Th. Weber, L. Young, Phys. Rev. Lett. **83**, 53 (1999).
15. M.A. Kornberg, J.E. Miraglia, Phys. Rev. A **53**, R3709 (1996).
16. J. Wang, J.H. McGuire, J. Burgdörfer, Y. Qiu, Phys. Rev. Lett. **77**, 1723 (1996).
17. M.A. Kornberg, J.E. Miraglia, Phys. Rev. A **48**, 3714 (1993).
18. M.A. Kornberg, J.E. Miraglia, in *The Physics of Electronic and Atomic Collisions*, edited by L.J. Dubé *et al.*, AIP Conference Proceedings, Vol. 360, pp. 763-771 (1995).
19. M.A. Kornberg, to be published.